Novel thermoresponsive polymer outperforming Pluronic® F127

Anna Constantinou
Imperial College London
Valeria Nele
Imperial College London
James Doutch
Science and Technology Facilities Council
Roman Moiseev
University of Reading https://orcid.org/0000-0002-4358-9981
Vitaliy Khutoryanskiy
University of Reading
Molly Stevens
Imperial College London https://orcid.org/0000-0002-7335-266X
Theoni Georgiou (t.georgiou@imperial.ac.uk)
Imperial College London https://orcid.org/0000-0003-4474-6931

Article

Keywords: Physically Crosslinked Networks, Formulation Science, Tissue Engineering, Gelation Concentration, Macroscale Gelling Behavior,

Posted Date: November 18th, 2020

DOI: https://doi.org/10.21203/rs.3.rs-104434/v1

Abstract

Thermoresponsive polymers featuring the appropriate combination of structural characteristics, i.e. architecture, composition, and molar mass (MM), can form physically crosslinked networks in a solvent upon changes in temperature. This fascinating class of polymers finds utility in various sectors such as formulation science and tissue engineering. Here, we report a novel thermoresponsive triblock terpolymer which out-performs the most commonly used and commercially available thermoresponsive polymer, Poloxamer P407 (also known as Pluronic® F127) in terms of gelation concentration. Specifically, the in-house synthesised polymer forms gels at lower concentrations that is an advantage in biomedical applications. To elucidate the differences in their macroscale gelling behaviour, we investigate their micellization via differential scanning calorimetry, and their nanoscale self-assembly behaviour in detail by means of small-angle neutron scattering by simultaneously recording their rheological properties (Rheo-SANS). Two different gelation mechanisms for the two polymers are revealed and proposed. Ex vivo gelation study upon intracameral injections demonstrated excellent potential for its application to improve drug residence in the eye.

Introduction

Thermoresponsive gels (TRGs) are 3-dimensional (3-D) networks of non-covalently interacting micelles that can reversibly turn to the solution phase as the stimulus (i.e. temperature) is removed.[1-5] For aqueous solutions, the crosslinking points are formed by hydrophobic junctions that are connected via hydrophilic bridges. This fascinating class of polymers has been extensively studied by polymer scientists, engineers, and biologists over the last decades, with the first systematic study on the subject dating back to 1984.[6] Particularly interesting are the TRGs that are formed upon a temperature increase; these polymers present a lower critical solution temperature (LCST), and their solubility decreases as function of temperature.[1]

TRGs with LCST behaviour have attracted much attention in the biomedical sector due to their reversible nature and their inherent ability of physical crosslinking without additional chemicals that might induce toxicity. They have been extensively studied as injectable gels either for tissue engineering (TE),[1, 7, 8] or to serve as drug delivery systems.[9, 10] In this concept, a prerequisite is a sol-gel transition between room temperature and physiological temperature. As a result, the solution phase can be loaded with cells and/or drugs at ambient temperature, in the case of TE and/or drug delivery application, respectively, and easily loaded into a syringe. Upon injection to physiological conditions, a hydrogel matrix is formed that traps the cells and/or drug molecules in place. In the case of drug delivery, the gel matrix provides sustained and topical release of the drug, which minimises undesired side-effects, caused by the systemic release. TRGs are most recently being investigated as 3-D printable (bio-)materials, such as implants.[11-15] The printing can be carried out either at room temperature or body temperature, depending on the desired application, and its feasibility relies on the shear-thinning properties of the hydrogel.

As previously mentioned, the synthesis and the applications of thermoresponsive polymers have been extensively reported.[16-28] Among these, poloxamer P407 is the most commonly used thermoresponsive polymer, owing to its commercial availability.[21, 29, 30] This copolymer is a member of the family of Pluronics®, which are ABA triblock copolymers with A and B units being ethylene glycol (EG) and propylene glycol (PG), respectively, i.e. EG_m-*b*-PG_n-*b*-EG_m; where m and n denote the degrees of polymerisation (DP) of EG and PG, respectively. It is known as Pluronic® F127 (registered tradename of BASF), and it consists of EG at 70 mol% and PG at 30 mol%, and its average molar mass (MM) is around 12600 g mol^{-1} ; its chemical structure is EG_{66}-*b*-PG_{99}-*b*-EG_{66} (the given DPs are approximate), and it is presented in Fig. 1a).[31-33] Poloxamers are widely used in industry as gelling, emulsifying and defoaming agents.[34-36] In the biomedical sector, and more specifically in the application of injectable gels, to the best of our knowledge, Pluronic® F127 is one of the two polymers that reached clinical trials, along with ReGel® (OncoGel: formulation with paclitaxel, NCT00479765, NCT00573131).[37-39] More specifically, Pluronic® F127 has been evaluated as a Simvastatin gel for the treatment of mucositis (20% gel, NCT03400475), and as a formulation with Pluronic® F68 as a Metronidazole vaginal gel for the treatment of bacterial vaginosis (20% F127/10% F68, NCT02365389).[38] In addition, its mixture with Pluronic® F68 is currently being trialled as a Timolol gel for the treatment of epistaxis (NCT04139018).[38] However, the minimum concentration at which Pluronic® F127 forms hydrogels is 15 w/w%, which might increase the cost of the application. Furthermore, depending on the concentration, Pluronic® F127 forms a gel or a very viscous liquid at room temperature, which makes it difficult to handle for some applications, such as those requiring injection through narrow needles. Therefore, there is a need for new thermoresponsive polymers able to overcome these challenges and that are easy to synthesise, thus rendering them suitable for industrial production.

To meet the current need, we report the design, synthesis and characterisation of a novel thermoresponsive polymer with a gelation concentration (C_{gel}) which is seven times lower than the one of Pluronic® F127. This copolymer is an ABC triblock terpolymer based on a novel combination of methacrylate units, in which B is the hydrophobic *n*-butyl methacrylate (BuMA), while A, and C are hydrophilic EG-based methacrylate units of different lengths. More specifically, A and C are penta- and di-(ethylene glycol) methyl ether methacrylate units, (PEGMA, and DEGMA, respectively); the latter shows cloud point (defined as the temperature at which the solution turns to cloudy, CP) at around 30 °C,[27, 40] while PEGMA presents CP at higher temperatures (~70°C).[40] Notably, this copolymer has been synthesised using Group Transfer Polymerisation (GTP), a polymerisation technique currently used in industry, due to its cost- and time-effectiveness and quantitative yields;[41-43] the latter eliminates the need of intermediate purification steps. Therefore, its mass production is certainly feasible. In order to fully harness its potential, an extensive characterisation of both self-assembly and rheological properties in aqueous milieu is necessary. More specifically, we performed visual tests, dynamic light scattering (DLS), and differential scanning calorimetry (DSC) to investigate its self-assembly and gelling behaviour. Furthermore, we performed rheology in conjunction with small-angle neutron scattering (Rheo-SANS), to scope out the macroscopic rheological behaviour and the self-assembly at the nanoscale at a range of

temperatures. We benchmarked our *in-house* synthesised polymer with Pluronic® F127. To the best of our knowledge, this is the first Rheo-SANS study on methacrylate ABC triblock terpolymers. The applicability of this novel polymer as an injectable formulation with sodium fluorescein was evaluated in comparison with Pluronic F127 in *ex vivo* experiments on intracameral injections into the bovine eyes.

Results

Design and Thermal Properties *in-house* Synthesised Polymer

In need of new thermoresponsive polymers, we designed and synthesised a triblock terpolymer which is based on a novel combination of methacrylate units. The triblock terpolymer has an ABC linear architecture, which has been shown to provide the best thermogelling properties, i.e. clear sol-gel transition without solubility issues, in the previously studied systems based on PEGMA-BuMA-DMAEMA;[16, 19] where DMAEMA stands for 2-(dimethylamino)ethyl methacrylate. This novel polymer consists of two hydrophilic compartments based on PEGMA (A block) and DEGMA (C block), which is also thermoresponsive close to physiological conditions (CP at 30 °C, depending on the MM), and a hydrophobic central block based on BuMA. Thus, its general chemical structure is $PEGMA_x$-*b*-$BuMA_y$-*b*-$DEGMA_z$, where x, y, and z are the DPs of PEGMA, BuMA, and DEGMA, respectively, as shown in Fig. 1b), along with the structure of Pluronic® F127. It is noteworthy that even though previous studies investigated polymers consisting of EG-based repeated units,[44, 45] this is the first time that this novel combination of repeated units is reported (patent published[46]). We believe that the substitution of DMAEMA units with DEGMA units will provide thermoresponsiveness, by avoiding any undesired effect of electrostatic interactions. In addition, the incorporation of BuMA units is beneficial, as it will promote self-assembly, while the incorporation of PEGMA units will balance the hydrophilicity, and thus solubility in aqueous media, while providing well-hydrated bridges between the micelles upon thermoresponse of DEGMA.

To ensure well-defined structural parameters, i.e. well-defined MM, and composition, we have implemented the synthesis via GTP, as these properties are crucial for controlling the thermoresponsive properties, i.e. gelation temperature (T_{gel}) and C_{gel}.[1] The gel permeation chromatography (GPC) traces of the triblock terpolymer (Supplementary Fig. S1) as well as the proton nuclear magnetic resonance (^{1}H NMR) spectra (Supplementary Fig. S2) reveal that we have successfully synthesised the triblock terpolymer with narrow MM distribution, indicated by the low dispersity value ($Đ$<1.2), and controllable MM and composition. The theoretical and experimental structural properties, i.e. MM, $Đ$, and composition are listed in Table S1.

To investigate the macroscopic differences in aqueous media between $PEGMA_x$-*b*-$BuMA_y$-*b*-$DEGMA_z$ and Pluronic® F127, we visually inspected the samples across a range of temperatures and concentrations and constructed the relative phase diagrams; the ones in phosphate buffered saline (PBS) are presented in Fig. 1c). The stable gel state, which is defined visually as the temperatures at which the sample does

not flow upon tube inversion, as indicated by the images in Fig. 1c), is of main importance. As extensively reported in the literature,[47-50] and shown in Fig. 1c) (left panel), the C_{gel} of Pluronic® F127 is 15 w/w%, and it forms gels at room temperature at 20 w/w% and 25 w/w%, which makes handling of the samples challenging, as previously discussed. On the other hand, as visible in Fig. 1c) (right panel), the *in-house* synthesised polymer, PEGMA$_x$-*b*-BuMA$_y$-*b*-DEGMA$_z$, is a runny solution at all concentrations tested at room temperature, which ensures homogeneity and ease in handling and injection. As the temperature is increased, a wide gelation area, shown approximately in black dashed line, is identified, with T_{gel} ranging from 32°C to 39°C, depending on the concentration. Most importantly, we report a novel polymer that gels at body temperature (denoted by black dotted line in Fig. 1c) at five times lower C_{gel} than Pluronic® F127. This is highly advantageous in terms of the cost-effectiveness of the application and low sample viscosity at room temperature upon administration. Interestingly, we observed a controlled decrease in T_{gel} by increasing the concentration from 2 w/w% to 25 w/w%, as opposed to the sudden decrease in T_{gel} for Pluronic® F127. Similar trends are observed in deionised water (see Fig. S3), with the T_{gel} (and C_{gel} for the PEGMA$_x$-*b*-BuMA$_y$-*b*-DEGMA$_z$) being slightly higher compared to the PBS solutions, which is attributed to the absence of ions in solutions.[47]

As previously mentioned, the solutions of the PEGMA$_x$-*b*-BuMA$_y$-*b*-DEGMA$_z$ are runny at room temperature, regardless the concentration, while the solutions of Pluronic® F127 are highly viscous, or gels at room temperature, depending on the concentration. To this end, we evaluated the injectability of their solutions at 15 w/w% in PBS, and it is proven that the injection rate of the polymer solution of PEGMA$_x$-*b*-BuMA$_y$-*b*-DEGMA$_z$ is at least one order of magnitude higher than to the one of Pluronic® F127, when the same force is applied (see Fig. S4 in Supplementary). Therefore, we demonstrate the ease in administration of the solution of PEGMA$_x$-*b*-BuMA$_y$-*b*-DEGMA$_z$, which is highly advantageous especially in the application of injectable gels, as injection of a sample of lower viscosity through narrow needles could be potentially less painful for the patient.

It is well-documented that DSC has been employed to monitor i) the micellisation, i.e. the self-assembly of unimers (free polymer chains) in micelles, the gelation, i.e. the formation of a 3-D network of interconnected micelles, and the cloud point, i.e. the phase separation, of polymer solutions.[50-56] Therefore, we employed DSC to record the changes in the thermal behaviour of the polymer solutions at 15 w/w% in PBS (C_{gel} for Pluronic® F127), and the results are presented in Fig.2; the repeated thermograms can be found in Fig. S5. As visible, a broad endothermic peak is present on the DSC thermogram of Pluronic® F127 (Fig. 2a)), with an onset temperature (T_{onset}) at 11.6±0.1 °C, and a maximum temperature (T_{max}) at 14.5±0.1 °C. This peak is indicative of the micellisation process of Pluronic® F127 caused by the de-hydration of the PG units, and it has been previously reported in the literature.[51, 54] The enthalpy of micellisation ($\Delta H_{micell.}$), calculated by the area of the endothermic peak, is 5.0±0.2 J/g (equal to 63 kJ/mol). Both the T_{max} and the $\Delta H_{micell.}$ for Pluronic® F127 are in a good agreement with previously reported values for similar systems.[50-54] As previously stated, the gelation

process is scarcely endothermic (i.e. almost athermal), and thus it has only been observed as a spike on the main peak at concentrations higher than the ones in the present study.[51, 54, 55] Studies on different systems other than Pluronics® recorded the phase separation at higher concentrations via DSC.[56] On the other hand, the DSC thermogram of PEGMA$_x$-*b*-BuMA$_y$-*b*-DEGMA$_z$ (Fig. 2 b)) shows no apparent changes up to 45°C, which could be due to the intrinsic micellisation, caused by the incorporation of the BuMA hydrophobic units within the polymer structure.

To confirm this hypothesis, we carried out DLS analysis on solutions of both Pluronic® F127 and PEGMA$_x$-*b*-BuMA$_y$-*b*-DEGMA$_z$ at 1 w/w% in PBS at 10°C and at room temperature (25°C), and the DLS histograms are shown as insets in Fig. 2. Concerning PEGMA$_x$-*b*-BuMA$_y$-*b*-DEGMA$_z$, we observed micelles at both temperatures, as the histograms almost overlap. In contrast, unimers, i.e. free polymer chains, are present in solutions of Pluronic® F127 at 10°C, as this temperature is lower than its micellisation temperature. By increasing the temperature to 25°C, a peak corresponding to micelles appears, the size of which is in agreement with the literature,[53, 57, 58] in addition to the peak which corresponds to the unimers. DLS at 25°C in deuterated phosphate buffered saline (D_2O/PBS), which is the solvent used during SANS, as it will be discussed in the following paragraphs, agrees with the results in PBS. The hydrodynamic diameters and the polydispersity (PDI) values, resulted from DLS analysis at 10°C and 25°C are listed in Table S2, and the corresponding DLS histograms by intensity and by number are presented in Figs. S6 and S7, respectively.

Rheological Properties and Self-Assembly behaviour

As the two polymers under investigation present clear differences in their macroscopic properties (i.e. T_{gel} and C_{gel}), in their thermal properties by calorimetry, and in their self-assembly behaviour by DLS, we used a state-of-the-art technique to gain further insights into their nanoscale self-assembly behaviour. Thus, we implemented Rheo-SANS, which is a powerful and non-destructive technique that records the scattering profiles of the polymeric ensembles at the nanoscale and the macroscopic rheological properties simultaneously, at a range of temperatures. In this study, we report and discuss the Rheo-SANS analysis of the polymer solutions at 15 w/w%, as this is the C_{gel} of Pluronic® F127. The solutions were prepared in D_2O/PBS to achieve good neutron contrast. The temperature ramp profiles of the PEGMA$_x$-*b*-BuMA$_y$-*b*-DEGMA$_z$ and Pluronic® F127 are presented in Fig.3 a) and b), respectively, while their SANS profiles at selected temperatures are shown in Fig.3 c) and d), respectively. The SANS profiles with the relative fit lines at all temperatures investigated can be found in Figs. S8 and S9, while the overlapped SANS profiles at selected temperatures are provided in Fig. S10, for direct comparison.

As corroborated by rheology (Fig. 3 a) and b)), both samples are in the liquid phase at room temperature, while they form gel as the temperature increases; T_{gel} is defined rheologically as the temperature at which the storage modulus G' exceeds the loss modulus G" (i.e. G'>G").[59] Interestingly, both samples are in the

gel state at body temperature ($T_{gel,\ Pluronic®\ F127}$ = 28°C, $T_{gel,\ PEGMAx\text{-}b\text{-}BuMAy\text{-}b\text{-}DEGMAz}$ = 32°C), while the gels are destabilised (G">G', T_{degel}) at 45°C, as expected by the visual tests (see Fig. 1 c) for PBS, and Fig. S11 for D_2O/PBS). The transition temperatures of PEGMA$_x$-*b*-BuMA$_y$-*b*-DEGMA$_z$ are in a good agreement with the values determined visually, both in PBS and D_2O/PBS, while the gelation area of Pluronic® F127 in D_2O/PBS is wider than in PBS, which is confirmed both visually and rheologically.

As can be seen in Fig. 3 c), and in more detail in Fig. S8 and S9, the *in-house* synthesised polymer, PEGMA$_x$-*b*-BuMA$_y$-*b*-DEGMA$_z$, presents different SANS profiles as the temperature increases, indicating changes in the morphology of its self-assembled structures. We used an elliptical cylinder model with a hardsphere form factor to fit the data up to 43°C, while a broad peak model was used to fit the data from 45°C; this temperature coincides with the T_{degel} by rheology.

From the SANS data, we inferred that the PEGMA$_x$-*b*-BuMA$_y$-*b*-DEGMA$_z$ formed micelles shaped as elliptical cylinders, whose best-fit values for the radius minor (blue dots) and the length (black dots) are shown in Fig. 4 (top panel, a)) as a function of the temperature. The best-fit radius axis ratio and volume fraction as a function of the temperature are shown in Fig. S12. As it is seen, the best-fit radius minor decreases from 47 Å to 44 Å, while the best-fit axis ratio increases from 1.3 to 1.5, as the temperature is increased from 23°C to 36°C. Interestingly, we observed a clear trend for the length of the cylinder, which increases significantly (from 126 Å to 460 Å), within the same temperature range; the fitting parameters of the elliptical cylinder above 36°C are not presented in Fig. 4, as the best-fit length was outside the limits of the SANS technique (2000 Å).

In order to fit the SANS data for PEGMA$_x$-*b*-BuMA$_y$-*b*-DEGMA$_z$ above the T_{degel}, we used a BroadPeak model, which provided the best-fit position of the Bragg peak.[60] This model is a combination of a Lorentzian-peak function and a power law decay and could suggest the presence of a bicontinuous structure[61] above the T_{degel}. As is seen in Fig. 4 (top panel, b)), the obtained Bragg peak position shifted from 0.044 Å^{-1} at 45°C to 0.059 Å^{-1} at 55°C. The d-spacing of this peak, calculated as d=2π/Q, is a characteristic distance between the scattering inhomogeneities,[61] and it decreases from d=144.21 Å and d=106.19 Å as the temperature increases from 45°C to 55°C as the sample proceeds from gel syneresis (i.e. disturbance of the gels, attributed to the inhomogeneity in the gel which causes increased internal stress, leading to the exclusion of solvent, firstly reported by Graham in 1864[62, 63]) to precipitation (i.e. clear separation into two phases – solid phase and liquid phase).

A proposed schematic of the elliptical cylinder structure adopted by PEGMA$_x$-*b*-BuMA$_y$-*b*-DEGMA$_z$ is also shown in Fig. 4 (top panel, c)), in which the hydrophilic PEGMA blocks, and the hydrophilic and thermoresponsive DEGMA blocks, shown in blue and green respectively, extend from the hydrophobic BuMA core, shown in orange, towards the aqueous environment.

The SANS profiles for Pluronic® F127, presented in Fig. 3 d), S9 and S10, are in a good agreement with the ones previously reported in the literature for concentrated solutions of the same polymer.[50, 64-67] We used the IGOR software to fit the scattering, as it was found to capture the scattering features/peaks best. From the SANS analysis, we observed the presence of globular structures, as indicated by the fitted power low value (P~3).

Interestingly, the scattering profiles of the solution of Pluronic® F127 present a series of peaks/shoulders at low Q values, which could be attributed to interparticle interference.[50, 65, 66] The first peak, which appears at Q ~ 0.035 $Å^{-1}$, is well-distinguishable at all temperatures (see Fig. 3) and it is a characteristic peak of highly concentrated solutions of Pluronic® F127, widely reported in the literature. We observed a shoulder at Q ~ 0.061 $Å^{-1}$ below 25 °C, at which the sample is in the solution state. At higher temperatures, a clear peak is detected at Q ~ 0.057 $Å^{-1}$, as can be seen in Fig. 3 d) middle and right, followed by two shoulders at Q = 0.067 $Å^{-1}$ and Q = 0.085 $Å^{-1}$ / 0.094 $Å^{-1}$ at higher temperatures. These features are also related to the interparticle interference and are associated with the formation of a polymer network.[50, 65, 66]

In addition to the series of peaks/shoulders at low Q values, a broad shoulder is present at Q ~ 0.12 $Å^{-1}$, which is due to intraparticle interferences.[65] We obtained a best-fit size core for the micellar core of approximately 4.4 nm, similarly to previously reported values.[65] This shoulder remains unchanged over the temperature range tested and it is an indication that the size of the self-assembled structures of Pluronic® F127 is not affected by the temperature, as previously reported.[66] This can also be seen in Fig. 4 (middle panel, a)), which presents the independence of the size of the core as a function of temperature. The suggested globular structure is shown in Fig. 4 (middle panel, b)), in which the well-hydrated PEG corona is shown in grey, and the compact hydrophobic core is illustrated as a black sphere.

It is worth noting that even though the position of the peaks, and thus the size of the globular structure is not affected by temperature, the scattering intensity clearly increases, indicating an increase in the volume fraction of the polymer. Thus, we confirm that the gelation of Pluronic® F127 is caused by an increase in the number of the globular structures, which has also been reported before in the literature.[67]

Our extensive Rheo-SANS analysis allowed us to reveal the differences in the nanoscale between $PEGMA_x$-*b*-$BuMA_y$-*b*-$DEGMA_z$, and Pluronic® F127. Thus, we conclude that the formation of gel by $PEGMA_x$-*b*-$BuMA_y$-*b*-$DEGMA_z$ is caused by the growth of the micelles, as indicated by the significant increase in their length (Fig. 4). On the other hand, the gelation of Pluronic® F127 is not caused by the change in the micelle size, but by the concentration of the micelles and the close packing, as indicated by the increase in volume fraction. The proposed gelation mechanisms are shown schematically in Fig. 4 (bottom), where the tricomponent system ($PEGMA_x$-*b*-$BuMA_y$-*b*-$DEGMA_z$) is shown in blue, orange, and green (top), while Pluronic® F127, which is a bicomponent system (EG_{66}-*b*-PG_{99}-*b*-EG_{66}), is presented in grey and black (bottom).

In order to evaluate the applicability of novel polymer in drug delivery a series of *ex vivo* experiments were performed using 15 wt % solutions, containing 1 mg/mL sodium fluorescein. In these experiments 15 wt % solution of Pluronic® F127 was used as a positive control (capable of forming gel at physiological temperature) and 15 wt % of Pluronic® F68 was used as a negative control (not capable of forming gel at physiological temperature). Solutions of control polymers were also containing 1 mg/mL sodium fluorescein. All these solutions were injected intracamerally into the anterior chamber of freshly excised bovine eyes thermostated at physiological temperature and the spreading of sodium fluorescein was monitored visually using video recording (see exemplar videos in Supplementary) and analysed using image analysis (Fig.5). As it was expected, the negative control formulation based on Pluronic® F68 exhibited very quick spreading of sodium fluorescein in the anterior chamber due to the absence of gelation. Both $PEGMA_x$-*b*-$BuMA_y$-*b*-$DEGMA_z$ and Pluronic® F127 formulations exhibited significantly slower spreading of sodium fluorescein ($p<0.05$) compared to Pluronic® F68, which is related to their gelation in the anterior chamber. This reduced spreadability of sodium fluorescein indicates the applicability of $PEGMA_x$-*b*-$BuMA_y$-*b*-$DEGMA_z$ for the potential design of injectable delivery systems to the anterior chamber, where longer drug residence will be of great importance. It is interesting to note that the formulation based on $PEGMA_x$-*b*-$BuMA_y$-*b*-$DEGMA_z$ shows a significantly slower spreadability of sodium fluorescein compared to Pluronic® F127 ($P<0.05$). This potentially indicates a further advantage of this polymer compared to Pluronic® F127.

In conclusion, we present a novel thermoresponsive terpolymer, namely $PEGMA_x$-*b*-$BuMA_y$-*b*-$DEGMA_z$, that gels at body temperature at a concentration which is five times lower than the one of the commercially available Pluronic® F127. While $PEGMA_x$-*b*-$BuMA_y$-*b*-$DEGMA_z$ inherently forms micelles due to the incorporation of permanently hydrophobic block, the micellisation of Pluronic® F127 is temperature-dependent, driven by the thermoresponse of the PG units. We used state-of-the-art characterisation techniques, such as DSC and Rheo-SANS, to probe the self-assembled nanostructures and gain insights into the gelation mechanism of $PEGMA_x$-*b*-$BuMA_y$-*b*-$DEGMA_z$. Thus, we conclude that $PEGMA_x$-*b*-$BuMA_y$-*b*-$DEGMA_z$ forms a gel due to the growth of the micelle structures to near cylindrical ensembles. On the other hand, the micelle size and shape adopted by Pluronic® F127 is independent of the temperature, but the volume fraction, and thus the population of globular structures increases as a function of temperature, thus leading to gel formation. The applicability of this novel methacrylate polymer for the use as an injectable intracameral formulation for ocular drug delivery is demonstrated.

Methods

Materials

All the monomers used in this study are commercially available and they were purchased from Sigma Aldrich Co Ltd., Irvine, United Kingdom (UK): PEGMA (MM = 300 g mol^{-1}, 95%), BuMA (99%), DEGMA (MM

= 188.22 g mol^{-1}, 95%). Chemicals needed for the monomer and solvent purification, polymer synthesis and characterisation as well as *ex vivo* intracameral injections were also purchased from Sigma Aldrich Co Ltd., Irvine, UK: calcium hydride (CaH_2, ≥ 90%, drying agent), basic aluminum oxide (Al_2O_3·KOH, acid remover), 2,2-diphenyl-1-picrylhydrazyl hydrate (DPPH, free-radical inhibitor), deuterated chloroform ($CDCl_3$, 99.8%, NMR solvent), triethylamine (Et_3N, HPLC grade, as additive in mobile phase for chromatography), methyl trimethylsilyl dimethylketene acetal (MTS, 95%, GTP initiator), tablets of phosphate buffered saline (PBS), Pluronic® F127, Pluronic® 68, sodium fluorescein and tetrahydrofuran (THF, HPLC grade, polymerisation solvent, ≥ 99.9%). The catalyst synthesis required the use of tetrabutylammonium hydroxide (40% in water) and benzoic acid, and they were purchased from Acros Organics (UK distributor – Fisher Scientific UK Ltd., Loughborough, UK). Acros Organics was also the provider of deuterium oxide (D_2O, 99.8%D). Fisher Scientific UK Ltd was also the provider of phosphate buffered saline (PBS) solution (10x solution, solvent for phase diagrams), and PBS tablets, *n*-hexane (precipitation solvent), and polytetrafluoroethylene (PTFE) hydrophilic syringe filters (0.45 µm pore size, 25 mm diameter). THF (HPLC grade, not stabilised, mobile phase in chromatography) was purchased from VWR International Ltd, Lutterworth, UK. Poly(methyl methacrylate) (PMMA) standard samples (MM = 2, 4, 8, 20, 50, and 100 kDa) that were used as calibrants for GPC system, were purchased from Fluka, Sigma Aldrich Co Ltd., Irvine, UK.

Purification of Starting Materials

The low MM monomers (BuMA and DEGMA) were purified in four steps: i) passing twice through basic alumina to remove the free-radical inhibitor, monomethyl ether hydroquinone, and any acidic components (i.e. methacrylic acid), ii) addition of DPPH to prevent undesired polymerisation, iii) addition of the desiccant CaH_2 and stirring for at least 3h to ensure dry conditions, and iv) vacuum distillation to remove DPPH and CaH_2/$Ca(OH)_2$. The high MM monomer, PEGMA, was purified in 2 steps as a solution in THF (50 v/v%) (Steps i) and iii). Direct filtration into the polymerisation flask was performed using PTFE filters to remove the CaH_2/$Ca(OH)_2$. The initiator (MTS) was vacuum distilled prior to use, while the catalyst (TBABB) was previously synthesised following a standard protocol,[68] and purified through re-crystallisation. The THF used during the polymerisation was purified using a solvent purification system, which is equipped with an activated alumina column (PureSolvTM Micro 100 Liter solvent purification system, purchased from Sigma Aldrich). All the glassware used for the vacuum distillations and polymerisation were dried overnight at 140°C.

Polymer Synthesis and Purification

The *in-house* synthesised triblock terpolymer, $PEGMA_x$-*b*-$BuMA_y$-*b*-$DEGMA_z$, was synthesised via sequential GTP. More specifically, around 10 mg of the catalyst, TBABB, was added in a one-neck round bottom flask, which was then sealed with a septum and purged with argon to ensure complete substitution of the atmosphere by inert argon gas. Subsequently, freshly purified THF (59 mL) was

syringed into the flask, followed by the addition of the MTS (0.55 mL, 0.5 g, 3 mmol). Three monomer additions were carried out as follows: i) PEGMA solution in THF (17 mL, 8.9g, 30 mmol), ii) BuMA (8.7 mL, 7.8 g, 55 mmol), and iii) DEGMA (5.5 mL, 5.5g, 29 mmol). The temperature changes after each monomer addition was monitored and recorded as follows: i) from 26.9 °C to 36.9 °C, ii) from 30.9 °C to 40.8 °C, and iii) from 32.9 °C to 37.9 °C, respectively. After each polymerisation step was completed, two aliquots (0.1 mL each) were withdrawn for GPC and ^{1}H NMR analysis. The polymer was purified and recovered via precipitation in cold *n*-hexane. The purification was completed by vacuum-drying at room temperature.

Gel Permeation Chromatography (GPC)

The successful sequential GTP was confirmed via GPC technique, which provides the MM values and the distributions of the final triblock terpolymer and its linear precursors. For this analysis, an Agilent SEC GPC system was used, which was purchased from Agilent technologies UK Ltd., Shropshire, UK. This system is equipped with an Agilent guard column (PL1110-1520, PLgel Mixed, dimensions [mm]: 50 × 7.5, particle size [µm]: 5), and a PSS (stands for Polymer Standard Service) SDV analytical linear M column (SDA083005LIM, dimensions [mm]: 300 × 8.00, particle size [µm]: 5, separation range [kg mol^{-1}]: 0.1 – 1000). The system also consists of a “1260 Iso” isocratic pump, which operates at 1 mL min^{-1} working flow rate. The differences in MM are detected by an Agilent 1250 refractive index (RI) detector, and the analysis was based on a linear calibration curve, as a result of six poly(methyl methacrylate) standard samples of MM values equal to 2, 4, 8, 20, 50 and 100 kg mol^{-1}. The GPC solvent pumped through the system was THF/Et_3N solution (95:5 v/v%). All the samples were prepared using the eluent solvent and they were filtered into GPC vials using PTFE filters (0.45 µm of pores diameter) before analysis. The GPC data were analysed using a PSS software (WinGPC UniChrom 8.2 software from PSS-Polymer).

The experimental MM values (resulted by GPC analysis) were compared to the theoretical ones ($MM_{theoretical}$), which were calculated using by summing the product of the MM of each monomer (MM_i) by its degree of polymerisation (DP_i). An additional MM of 100 g mol^{-1} was added to the result to take into consideration the part of the initiator, MTS, that stays on the polymer chain after the GTP is completed. Simply stated, the theoretical MM values can be calculated using the Equation 1 below:

$$MM_{theoretical}\ (g\ mol^{-1}) = (\sum_i MM_i \times DP_i) + 100.$$

Nuclear Magnetic Resonance (NMR) Spectroscopy

The experimental compositions of the final terpolymer and its linear precursors were confirmed by ^{1}H NMR spectroscopy. The NMR samples were prepared by dissolving the dried polymer samples in deuterated chloroform. The solutions were analysed by using a a 400-MHz Avance Bruker NMR spectrometer from Bruker (Bruker, UK Ltd., Coventry, UK). The data were analysed using a MestReNova software (Version: 11.0.0-17609 ©2016 Mestrelab Research S.L.).

The prove the successful GTP, the experimental weight percentages were calculated by analysing the NMR results and they were compared to the targeted ones. The following peaks were used for the analysis: i) for PEGMA and DEGMA, which are both EG-based methacrylate units, the distinctive peak of their methoxy group ($C\mathbf{H_3}O-$) at 3.35 ppm was used, and ii) for BuMA, the peak of the methylene group closest to the ester was used ($CH_3CH_2CH_2C\mathbf{H_2}O-$), which appears at 3.9 ppm.

Dynamic Light Scattering (DLS)

The diluted aqueous solutions (1 w/w%) of both PEGMA$_x$-*b*-BuMA$_y$-*b*-DEGMA$_z$ and the Pluronic® F127 were analysed using a Zetasizer Nano ZSP from Malvern Instruments Ltd. (Malvern, UK). The polymer solutions were tested under the following solvents: i) PBS, and ii) D_2O/PBS. The polymer solutions were tested without any further processing, i.e. filtration, to ensure that a direct comparison between the different techniques of determining the size can be made. The DLS experiments were performed at room temperature (25 °C), while in the case of PBS solutions, the samples were also tested at 10 °C. In all the cases, the scattered light was collected at a backscatter angle of 173°. Each sample was analysed three times and the results reported are the mean hydrodynamic diameters (d_h) that corresponds to the maximum of the peak by intensity, and by number. The data were analysed using a Zetasizer software (version 7.11) from Malvern Polyanalytical.

Differential Scanning Calorimetry (DSC)

15 w/w% solutions in PBS of PEGMA$_x$-*b*-BuMA$_y$-*b*-DEGMA$_z$ and Pluronic® F127 were prepared three times (three polymer solutions for each polymer). Each sample was analysed using DSC three times (nine results per polymer). For the analysis, the samples were placed in T-zero® style hermetic aluminium pans (purchased from Thermal Instruments Ltd., UK). The DSC was performed using the DSC Q2000 (TA Instruments, UK) at a heating rate of 5°C/min between 2 and 60°C under nitrogen atmosphere. The obtained data were analysed using Universal Analysis 2000 software (TA Instruments Version 4.5A).

Rheology-Small Angle Neutron Scattering (Rheo-SANS)

The polymer solutions at 15 w/w% D_2O/PBS of both $PEGMA_x$-*b*-$BuMA_y$-*b*-$DEGMA_z$ and Pluronic® F127 were investigated by Rheo-SANS. More specifically, the self-assembly as well as the rheological properties of the samples were tested at a range of temperatures. This experiment was performed at the time of flight SANS instrument ZOOM at the ISIS pulsed neutron source at the Rutherford Appleton Laboratory (Didcot, UK), using source to sample and sample to detector distance of 4m, and wavelengths 1.5 – 16.5 Å. For this experiment, an Anton Paar rheometer (Physica MCR501) equipped with a special Searle-Couette (rotating stator) measuring geometry, manufactured in Grade-V Titanium. The temperature ramp measurements were performed at constant strain (γ = 1%), and constant angular frequency (ω = 1 $rads^{-1}$), which are within the linear viscoelastic area (see Fig. S13). Data were reduced using MantidPlot,[69] and the resulted SANS curves were fitted using the following software: i) SasView software (version 5.0) for the novel polymer and ii) IGOR software for Pluronic® F127.[70]

Ex vivo experiments with intracameral injections

Bovine eyes were delivered from a local abattoir within three hours. Appropriate randomisation in experiments with intracameral injections was achieved by labelling each eye with a number and placing another set of labels with the same figures in the non-transparent black bag. The randomisation was done by means of pulling labels out of the bag randomly.

15 wt% polymer solutions of $PEGMA_x$-*b*-$BuMA_y$-*b*-$DEGMA_z$, Pluronic® F127 and Pluronic® F68 were prepared by dissolving the required amounts of each polymer in 1 mg/mL sodium fluorescein in PBS solution and stirred overnight at 4°C to form clear solutions. The $PEGMA_x$-*b*-$BuMA_y$-*b*-$DEGMA_z$ solution in PBS containing 1 mg/mL sodium fluorescein was kept in an incubator at 33 °C for 20 minutes prior to the intracameral injections. The solution of Pluronic® F127 in PBS containing 1 mg/mL sodium fluorescein was stored at room temperature for 20 minutes before the injection. Solution of Pluronic® F68 in PBS containing 1mg/mL sodium fluorescein was kept in the fridge at 4 °C for 20 minutes prior to the injection.

All nine *ex-vivo* bovine eyeballs were kept at 37 °C (human body temperature) for at least 40 minutes prior to the injection in the anterior chamber (0.05 mL; 21-gauge needle, 1mL syringe). Three runs for each polymer solution were performed within the incubator at 37 °C. All the experiments were recorded for 3.5 minutes using iPhone XS. All experiments were performed in triplicate and data were analysed using GraphPad Prism 8.0.2 software. where $p < 0.05$ was used as the statistical significance criterion. The significance of the calculated mean values ± standard deviations was assessed using one-way analysis of variance (ANOVA) followed by Bonferroni *post hoc* test, where $p < 0.05$ was selected as the statistical significance criterion.

Then, the extent of fluorophore spreading in the anterior chamber was evaluated using ImageJ software (version 1.50i) at different time points (0, 1, 1.5, 2, 2.5 and 3 minutes) starting from the moment of the complete pull of the needle out of the anterior chamber for each run of each polymer solution tested.

Injectability experiments

The injectability of the solutions of $PEGMA_x$-*b*-$BuMA_y$-*b*-$DEGMA_z$ and Pluronic® F127 at 15 w/w% in PBS was evaluated at room temperature. To accomplish this, a 2 mL gas-tight glass syringe (Cadence Science, Inc.) containing the solution, fitted with hypodermic needles, was placed vertically, as shown schematically in Fig. S4 a). The following needles (diameter x length, mm) were used: 23G 1” (0.6 x 25, fine-ject®), 24G 1” (0.55 x 25, fine-ject®), 25G 1” (0.5x 25, fine-ject®), 26G 1” (0.45 x 25, fine-ject®), and 27G 3/4” (0.4 x 20 henke-ject®). Two different weights were placed on top of the needle, 200 g and 500 g, with a resulting force applied for the injection equal to 2.0 N and 4.9 N, respectively. The time of injection of 0.5 mL of solution was measured and the injection rate (mL/min) was calculated. Each experiment was repeated six times and the standard error was calculated.

References

1. Constantinou, A. P. & Georgiou, T. K. Tuning the gelation of thermoresponsive gels. *Eur. Polym. J.* **78**, 366-375 (2016).
2. Constantinou, A. P. & Georgiou, T. K. in *Temperature-Responsive Polymers: Chemistry, Properties, and Applications* (eds Khutoryanskiy, V. V. & Georgiou, T. K.) 35-65 (John Wiley & Son Ltd, United Kingdom, 2018).
3. Ward, M. A. & Georgiou, T. K. Thermoresponsive polymers for biomedical applications. *Polymers* **3**, 1215-1242 (2011).
4. Klouda, L. & Mikos, A. G. Thermoresponsive hydrogels in biomedical applications. *Eur. J. Pharm. Biopharm.* **68**, 34-45 (2008).
5. Klouda, L. Thermoresponsive hydrogels in biomedical applications: A seven-year update. *Eur. J. Pharm. Biopharm.* **97**, 338-349 (2015).
6. Vadnere, M., Amidon, G., Lindenbaum, S. & Haslam, J. L. Thermodynamic studies on the gel-sol transition of some pluronic polyols. *Int. J. Pharm.* **22**, 207-218 (1984).
7. Place, E. S., George, J. H., Williams, C. K. & Stevens, M. M. Synthetic polymer scaffolds for tissue engineering. *Chem. Soc. Rev.* **38**, 1139-1151 (2009).
8. Gutowska, A., Jeong, B. & Jasionowski, M. Injectable gels for tissue engineering. *Anat. Rec.* **263**, 342-349 (2001).
9. Bobbala, S., Tamboli, V., McDowell, A., Mitra, A. K. & Hook, S. Novel Injectable Pentablock Copolymer Based Thermoresponsive Hydrogels for Sustained Release Vaccines. *AAPS Journal* **18**, 261-269 (2016).
10. Wu, Q. *et al*. Mannan loaded biodegradable and injectable thermosensitive PCL-PEG-PCL hydrogel for vaccine delivery. *Soft Materials* **10**, 472-486 (2012).

11. Feilden, E., Blanca, E. G., Giuliani, F., Saiz, E. & Vandeperre, L. Robocasting of structural ceramic parts with hydrogel inks. *Journal of the European Ceramic Society* **36**, 2525-2533 (2016).
12. Rocha, V. G. *et al*. Multimaterial 3D Printing of Graphene-Based Electrodes for Electrochemical Energy Storage Using Thermoresponsive Inks. *ACS Appl. Mater. Interfaces* **9**, 37136-37145 (2017).
13. Suntornnond, R., An, J. & Chua, C. K. Bioprinting of Thermoresponsive Hydrogels for Next Generation Tissue Engineering: A Review. *Macromol. Mater. Eng.* **302**, 1600266 (2017).
14. Zhang, M. *et al*. Dual-Responsive Hydrogels for Direct-Write 3D Printing. *Macromolecules* **48**, 6482-6488 (2015).
15. Skardal, A. & Atala, A. Biomaterials for Integration with 3-D Bioprinting. *Ann. Biomed. Eng.* **43**, 730-746 (2015).
16. Constantinou, A. P., Zhao, H., McGilvery, C. M., Porter, A. E. & Georgiou, T. K. A Comprehensive Systematic Study on Thermoresponsive Gels: Beyond the Common Architectures of Linear Terpolymers. *Polymers* **9**, 31 (2017).
17. Constantinou, A. P. & Georgiou, T. K. Thermoresponsive gels based on ABC triblock copolymers: effect of the length of the PEG side group. *Polym. Chem.* **7**, 2045-2056 (2016).
18. Constantinou, A. P., Sam-Soon, N., Carroll, D. R. & Georgiou, T. K. Thermoresponsive Tetrablock Terpolymers: Effect of Architecture and Composition on Gelling Behavior. *Macromolecules* **51**, 7019-7031 (2018).
19. Ward, M. A. & Georgiou, T. K. Thermoresponsive terpolymers based on methacrylate monomers: Effect of architecture and composition. *J. Polym. Sci. A Polym. Chem.* **48**, 775-783 (2010).
20. Ward, M. A. & Georgiou, T. K. Thermoresponsive triblock copolymers based on methacrylate monomers: effect of molecular weight and composition. *Soft Matter* **8**, 2737-2745 (2012).
21. Müller, M., AU - Becher, J., AU - Schnabelrauch, M. & AU - Zenobi-Wong, M. Printing Thermoresponsive Reverse Molds for the Creation of Patterned Two-component Hydrogels for 3D Cell Culture. *JoVE*, e50632 (2013).
22. Strappe, P. M., Hampton, D. W., Cachon-Gonzalez, B., Fawcett, J. W. & Lever, A. Delivery of a lentiviral vector in a Pluronic F127 gel to cells of the central nervous system. *European Journal of Pharmaceutics and Biopharmaceutics* **61**, 126-133 (2005).
23. Bobbala, S., Gibson, B., Gamble, A. B., McDowell, A. & Hook, S. Poloxamer 407-chitosan grafted thermoresponsive hydrogels achieve synchronous and sustained release of antigen and adjuvant from single-shot vaccines. *Immunol. Cell Biol.* **96**, 656-665 (2018).
24. Hoogenboom, R. Poly(2-oxazoline)s: A Polymer Class with Numerous Potential Applications. *Angewandte Chemie International Edition* **48**, 7978-7994 (2009).
25. Hoogenboom, R. & Schlaad, H. Thermoresponsive poly(2-oxazoline)s, polypeptoids, and polypeptides. *Polym. Chem.* **8**, 24-40 (2017).
26. Lanzalaco, S. & Armelin, E. Poly(N-isopropylacrylamide) and Copolymers: A Review on Recent Progresses in Biomedical Applications. *Gels* **3** (2017).

27. Lutz, J., Akdemir, Ö & Hoth, A. Point by Point Comparison of Two Thermosensitive Polymers Exhibiting a Similar LCST: Is the Age of Poly(NIPAM) Over? *J. Am. Chem. Soc.* **128**, 13046-13047 (2006).
28. Al Khateb, K. *et al*. In situ gelling systems based on Pluronic F127/Pluronic F68 formulations for ocular drug delivery. *International Journal of Pharmaceutics* **502**, 70-79 (2016).
29. Dumortier, G., Grossiord, J. L., Agnely, F. & Chaumeil, J. C. A review of poloxamer 407 pharmaceutical and pharmacological characteristics. *Pharm. Res.* **23**, 2709-2728 (2006).
30. Edsman, K., Carlfors, J. & Petersson, R. Rheological evaluation of poloxamer as an in situ gel for ophthalmic use. *Eur. J. Pharm. Sci* **6**, 105-112 (1998).
31. Almeida, M., Magalhães, M., Veiga, F. & Figueiras, A. Poloxamers, poloxamines and polymeric micelles: Definition, structure and therapeutic applications in cancer. *Journal of Polymer Research* **25**, 31 (2017).
32. Thakur, R. R. S., Fallows, S. J., McMillan, H. L., Donnelly, R. F. & Jones, D. S. Microneedle-mediated intrascleral delivery of in situ forming thermoresponsive implants for sustained ocular drug delivery. *J. Pharm. Pharmacol.* **66**, 584-595 (2014).
33. Kolesky, D. B. *et al*. 3D Bioprinting of Vascularized, Heterogeneous Cell-Laden Tissue Constructs. *Adv Mater* **26**, 3124-3130 (2014).
34. Gardener, S. & Jones, G. J. A New Solidifying Agent for Culture Media Which Liquefies on Cooling. *Microbiology* **130**, 731-733 (1984).
35. Ng, S. M. & Wieckowski, S. Stable hydrogen peroxide dental gel. **4,839,156** (1989).
36. Patel, K. *et al*. Salt-Induced Micellization of Pluronic F88 in Water. *J. Dispersion Sci. Technol.* **29**, 748-755 (2008).
37. Elstad, N. L. & Fowers, K. D. OncoGel (ReGel/paclitaxel) - Clinical applications for a novel paclitaxel delivery system. *Adv. Drug Deliv. Rev.* **61**, 785-794 (2009).
38. https://clinicaltrials.gov/.
39. Pitto-Barry, A. & Barry, N. P. E. Pluronic® block-copolymers in medicine: from chemical and biological versatility to rationalisation and clinical advances. *Polym. Chem.* **5**, 3291-3297 (2014).
40. Lutz, J. Polymerization of oligo(ethylene glycol) (meth)acrylates: Toward new generations of smart biocompatible materials. *J. Polym. Sci. A Polym. Chem.* **46**, 3459-3470 (2008).
41. Webster, O. W., Hertler, W. R., Sogah, D. Y., Farnham, W. B. & RajanBabu, T. V. Group-transfer polymerization. 1. A new concept for addition polymerization with organosilicon initiators. *J. Am. Chem. Soc.* **105**, 5706-5708 (1983).
42. Patrickios, C. S., Lowe, A. B., Armes, S. P. & Billingham, N. C. ABC triblock polymethacrylates: Group transfer polymerization synthesis of the ABC, ACB, and BAC topological isomers and solution characterization. *J. Polym. Sci. Part A* **36**, 617-631 (1998).
43. Webster, O. W. in *New Synthetic Methods* 1-34 (Springer Berlin Heidelberg, Berlin, Heidelberg, 2004).

44. Lutz, J., Weichenhan, K., Akdemir, Ö & Hoth, A. About the Phase Transitions in Aqueous Solutions of Thermoresponsive Copolymers and Hydrogels Based on 2-(2-methoxyethoxy)ethyl Methacrylate and Oligo(ethylene glycol) Methacrylate. *Macromolecules* **40**, 2503-2508 (2007).
45. Lutz, J. & Hoth, A. Preparation of Ideal PEG Analogues with a Tunable Thermosensitivity by Controlled Radical Copolymerization of 2-(2-Methoxyethoxy)ethyl Methacrylate and Oligo(ethylene glycol) Methacrylate. *Macromolecules* **39**, 893-896 (2006).
46. Georgiou, T. & Constantinou, A. Polymers. **PCT/GB20 19/052686** (2020).
47. Malmsten, M. & Lindman, B. Self-assembly in aqueous block copolymer solutions. *Macromolecules* **25**, 5440-5445 (1992).
48. Malmsten, M. & Lindman, B. Effects of homopolymers on the gel formation in aqueous block copolymer solutions. *Macromolecules* **26**, 1282-1286 (1993).
49. Li, X. & Hyun, K. Rheological study of the effect of polyethylene oxide (PEO) homopolymer on the gelation of PEO-PPO-PEO triblock copolymer in aqueous solution. *Korea-Australia Rheology Journal* **30**, 109-125 (2018).
50. Shriky, B. *et al*. Pluronic F127 thermosensitive injectable smart hydrogels for controlled drug delivery system development. *Journal of Colloid and Interface Science* **565**, 119-130 (2020).
51. Branca, C., Khouzami, K., Wanderlingh, U. & D'Angelo, G. Effect of intercalated chitosan/clay nanostructures on concentrated pluronic F127 solution: A FTIR-ATR, DSC and rheological study. *Journal of Colloid and Interface Science* **517**, 221-229 (2018).
52. Wanka, G., Hoffmann, H. & Ulbricht, W. Phase Diagrams and Aggregation Behavior of Poly(oxyethylene)-Poly(oxypropylene)-Poly(oxyethylene) Triblock Copolymers in Aqueous Solutions. *Macromolecules* **27**, 4145-4159 (1994).
53. Pham Trong, L. C., Djabourov, M. & Ponton, A. Mechanisms of micellization and rheology of PEO–PPO–PEO triblock copolymers with various architectures. *Journal of Colloid and Interface Science* **328**, 278-287 (2008).
54. Barba, A. A. *et al*. Investigation of Pluronic© F127–Water solutions phase transitions by DSC and dielectric spectroscopy. *J Appl Polym Sci* **114**, 688-695 (2009).
55. Yu, G. *et al*. Micellisation and gelation of triblock copoly(oxyethylene/oxypropylene/oxyethylene), F127. *J. Chem. Soc. , Faraday Trans.* **88**, 2537-2544 (1992).
56. Aravopoulou, D. *et al*. Comparative Investigation of the Thermoresponsive Behavior of Two Diblock Copolymers Comprising PNIPAM and PMDEGA Blocks. *J Phys Chem B* **122**, 2655-2668 (2018).
57. Alexandridis, P. & Alan Hatton, T. Poly(ethylene oxide)-poly(propylene oxide)-poly(ethylene oxide) block copolymer surfactants in aqueous solutions and at interfaces: thermodynamics, structure, dynamics, and modeling. *Colloids and Surfaces A: Physicochemical and Engineering Aspects* **96**, 1-46 (1995).
58. Lin, Y. & Alexandridis, P. Temperature-Dependent Adsorption of Pluronic F127 Block Copolymers onto Carbon Black Particles Dispersed in Aqueous Media. *J Phys Chem B* **106**, 10834-10844 (2002).

59. Cheng, V., Lee, B. H., Pauken, C. & Vernon, B. L. Poly(N-isopropylacrylamide-co-poly(ethylene glycol))-acrylate simultaneously physically and chemically gelling polymer systems. *J Appl Polym Sci* **106**, 1201-1207 (2007).
60. Nele, V. *et al*. Effect of Formulation Method, Lipid Composition, and PEGylation on Vesicle Lamellarity: A Small-Angle Neutron Scattering Study. *Langmuir* **35**, 6064-6074 (2019).
61. ftp.ncnr.nist.gov › kline.
62. Kunitz, M. SYNERESIS AND SWELLING OF GELATIN. *J. Gen. Physiol.* **12**, 289-312 (1928).
63. Van Dijk, H. J. M., Walstra, P. & Schenk, J. Theoretical and experimental study of one-dimensional syneresis of a protein gel. *The Chemical Engineering Journal* **28**, B43-B50 (1984).
64. Sharma, P. K. & Bhatia, S. R. Effect of anti-inflammatories on Pluronic® F127: micellar assembly, gelation and partitioning. *International Journal of Pharmaceutics* **278**, 361-377 (2004).
65. Li, Y., Shi, T., Sun, Z., An, L. & Huang, Q. Investigation of Sol–Gel Transition in Pluronic F127/D2O Solutions Using a Combination of Small-Angle Neutron Scattering and Monte Carlo Simulation. *J Phys Chem B* **110**, 26424-26429 (2006).
66. Prud'homme, R. K., Wu, G. & Schneider, D. K. Structure and Rheology Studies of Poly(oxyethylene–oxypropylene–oxyethylene) Aqueous Solution. *Langmuir* **12**, 4651-4659 (1996).
67. Mortensen, K. & Talmon, Y. Cryo-TEM and SANS Microstructural Study of Pluronic Polymer Solutions. *Macromolecules* **28**, 8829-8834 (1995).
68. Dicker, I. B. *et al*. Oxyanions catalyze group-transfer polymerization to give living polymers. *Macromolecules* **23**, 4034-4041 (1990).
69. Arnold, O. *et al*. Mantid—Data analysis and visualization package for neutron scattering and μ SR experiments. *Nuclear Instruments and Methods in Physics Research Section A: Accelerators, Spectrometers, Detectors and Associated Equipment* **764**, 156-166 (2014).
70. UTK, UMD, NIST, ORNL, ISIS, ESS, ILL, ANSTO, TU Delft, DLS. SasView. **5.0**.

Declarations

Acknowledgments

A.P.C. acknowledges the Engineering and Physical Sciences Research Council (EPSRC) for the Doctoral Prize Fellowship (EP/M506345/1) as well as the EPSRC Impact Acceleration Grant EP/R511547/1. V.N. acknowledges the Ermenegildo Zegna Founder's Scholarship program. V.N. and M.M.S. acknowledge support from the Rosetrees Trust. RVM acknowledges the University of Reading International Scholarship.The Rheo-SANS experiments were performed at the ISIS Neutron and Muon Source at the STFC Rutherford Appleton Laboratory, UK, and they were supported by a beamtime allocation from the Science and Technology Facilities Council (1910285). The SANS analysis has been carried out using the SasView software,which was originally developed under the NSF award DMR-0520547. The software contains code the development of which was funded by the European Union's Horizon 2020 research and innovation programme under the SINE2020 project, grant agreement 654000.

Authors Contributions

A.P.C. designed, synthesised, purified and characterised the novel polymer, $PEGMA_x$-*b*-$BuMA_y$-*b*-$DEGMA_z$, via GPC, NMR spectroscopy, visual tests, rheology, DLS, characterised the Pluronic® F127 by visual tests, rheology and DLS, assisted with Rheo-SANS experiments and the SANS fitting analysis, and with the DSC analysis, plotted the graphs and has written the first draft of the manuscript, and is responsible for reviewing and editing the final manuscript. V.N. assisted with Rheo-SANS experiments and the SANS fitting analysis. J.J.D. is the responsible in the ICIS facilities and he guided and supervised the Rheo-SANS experiments and the SANS fitting analysis and has also assisted with the analysis of the data of Pluronic® F127 using IGOR software. R.V.M carried out the DSC experiments, and the *ex vivo* experiments with intracameral injections, and has also performed the analysis related to the *ex vivo* experiments. V.V.K. is the supervisor of R.V.M. and he provided access to the DSC equipment and general supervision on the DSC experiments and on the *ex vivo* experiments with intracameral injections. M.M.S. is the supervisor of V.N., who assisted and provided her expertise on SANS technique. T.K.G. is the project's supervisor, administrator and organiser and assisted with the Rheo-SANS experiments.

Competing Interests

APC and TKG report that part of this work, regarding the novel chemistry of the materials and their promising thermoresponsive properties have been patented.[46]

Materials and Correspondence

Correspondence and material requests should be addressed to T.K.G.

Figures

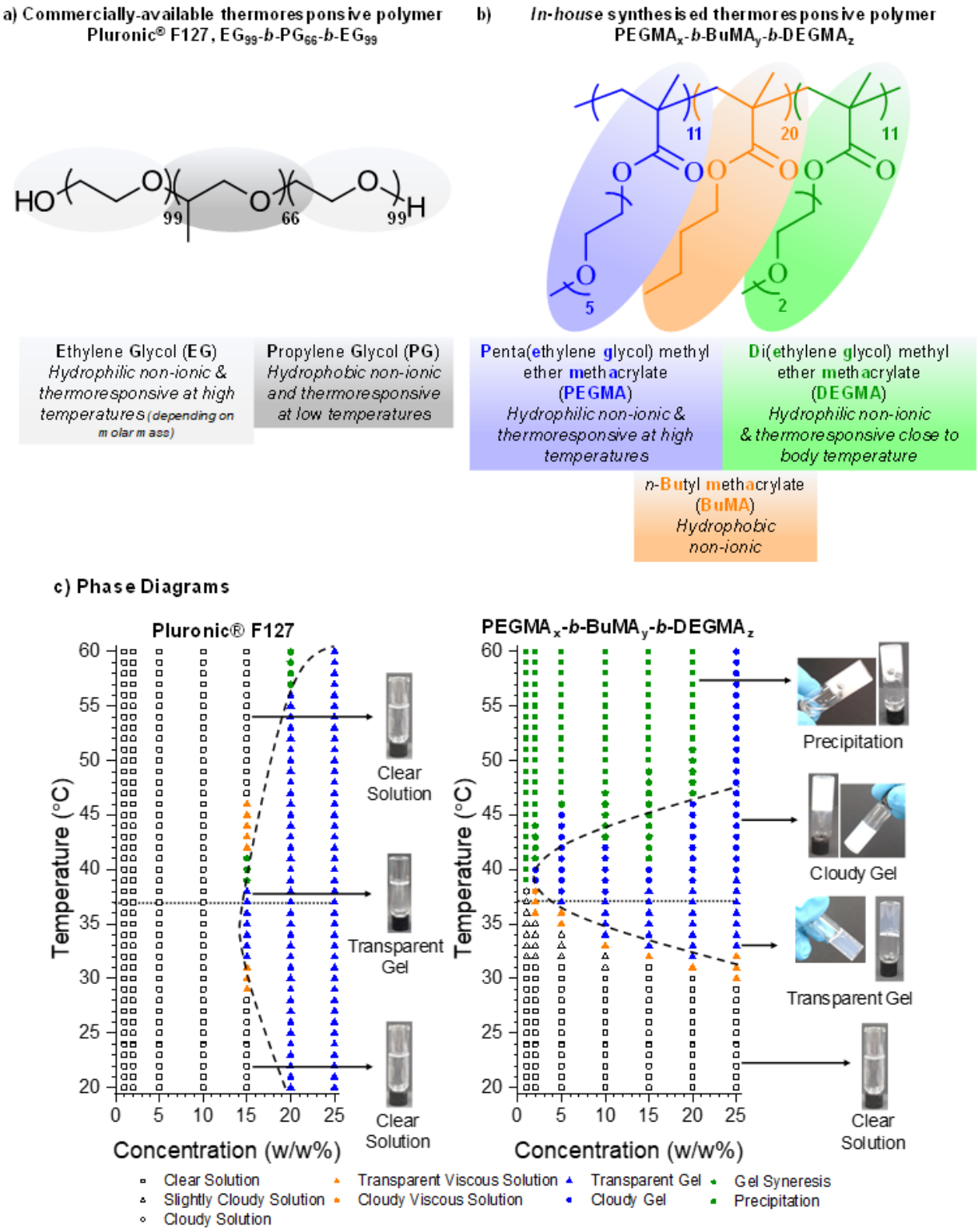

Figure 1

a) Chemical structures of the commercially available thermoresponsive polymer, namely Pluronic® F127, b) chemical structure of the in-house synthesised polymer, PEGMAx-b-BuMAy-b-DEGMAz, and c) phase diagrams in phosphate buffered saline (PBS) of Pluronic® F127 (left) and the PEGMAx-b-BuMAy-b-DEGMAz (right). Images of the main results for sol-gel transitions are also presented. The different phases are symbolised as follows: i) runny solution phase in white (square, triangle and circle correspond

to clear, slightly cloudy and cloudy states, respectively), ii) viscous solution phase in orange (triangle and circle correspond to transparent and cloudy states, respectively), iii) stable gel phase in blue (triangle and circle correspond to transparent and cloudy gels, respectively, and iv) two-phases in green (rhombus and square correspond to gel syneresis and precipitation, respectively). The gelation area is approximately shown in black dashed line, while body temperature is indicated by black dotted line. Note: the degrees of polymerisation (DPs) for Pluronic® F127 are approximate, while the DPs of PEGMAx-b-BuMAy-b-DEGMAz correspond to the targeted values.

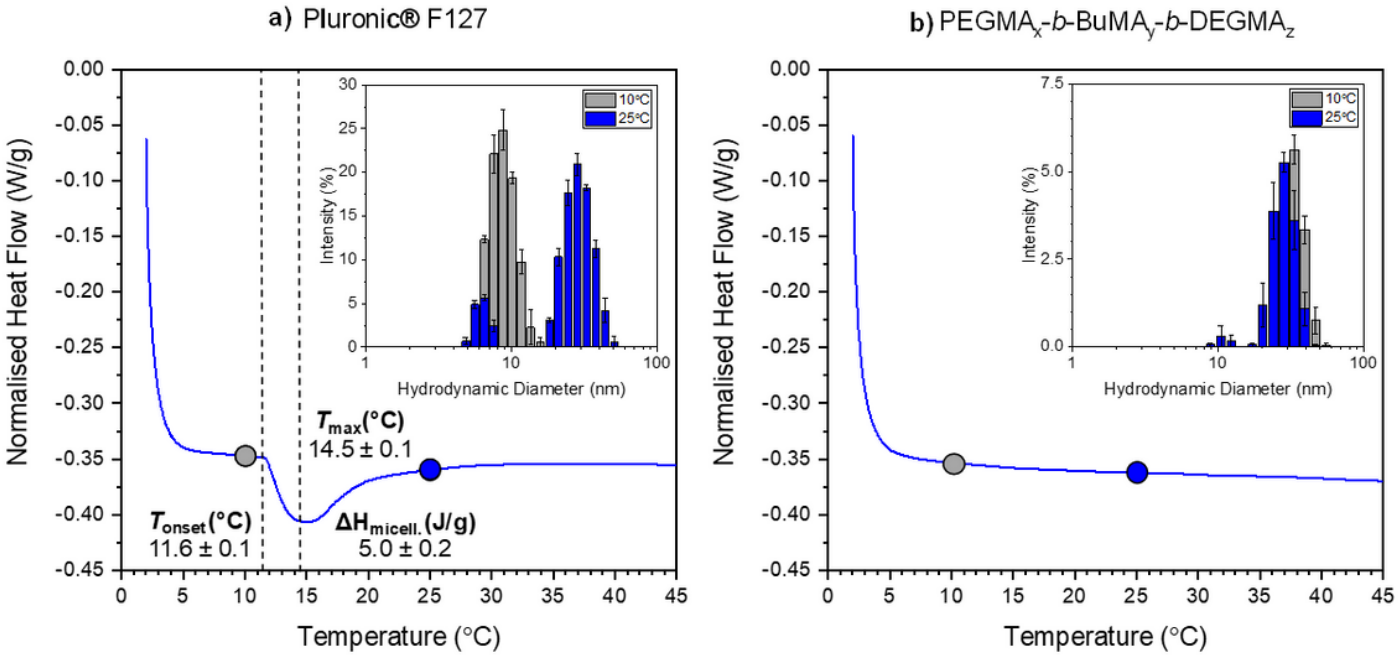

Figure 2

DSC thermograms of 15 w/w% polymer solutions in phosphate buffered saline (PBS) of a) Pluronic® F127, and b) PEGMAx-b-BuMAy-b-DEGMAz. The DLS histograms of 1 w/w% polymer solutions in phosphate buffered saline (PBS) at 10°C (grey) and 25°C (blue) are also presented as insets.

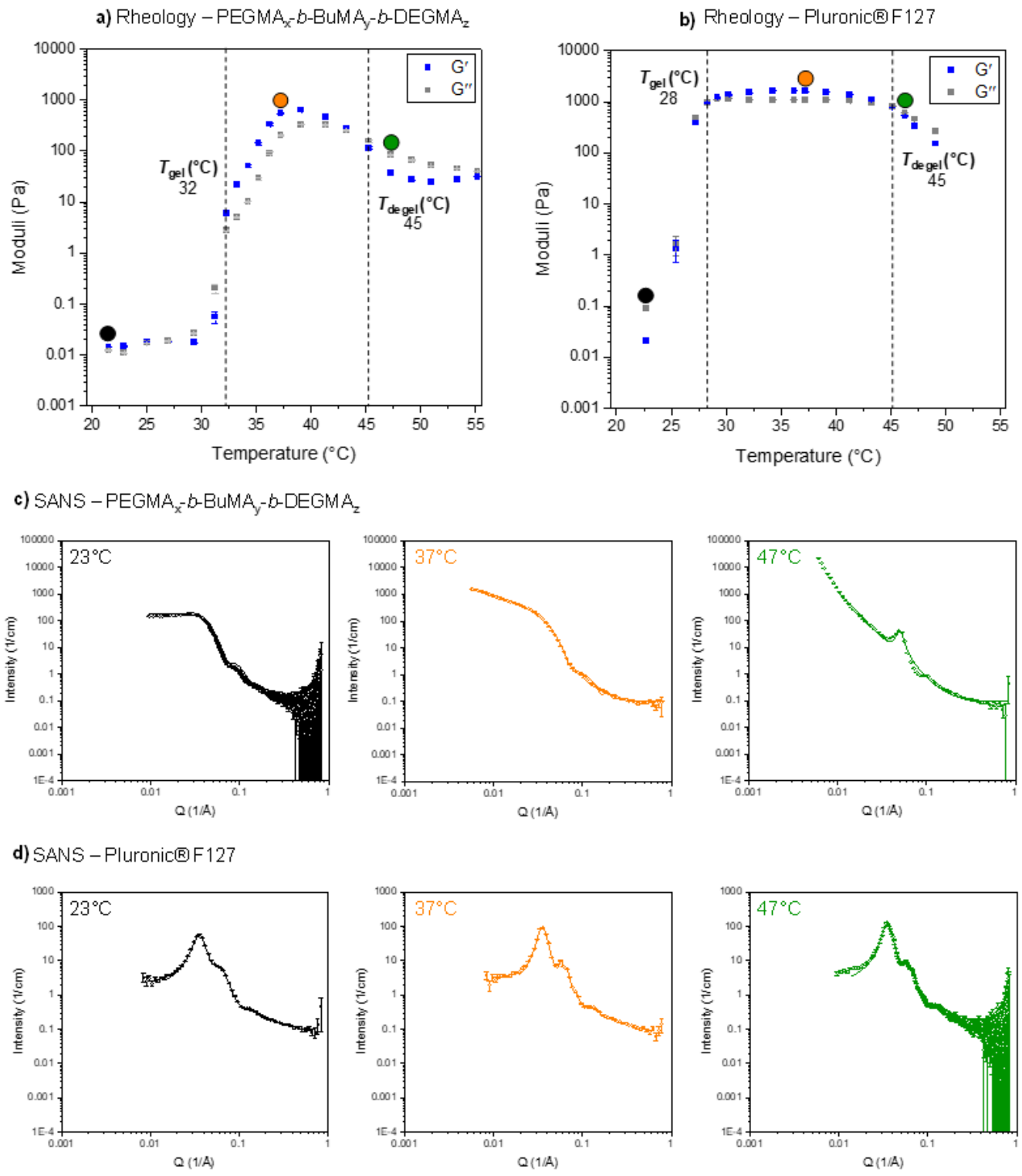

Figure 3

Rheo-SANS data of 15 w/w% solutions in deuterated phosphate buffered saline (D2O/PBS): i) temperature sweep rheological measurements on a) PEGMAx-b-BuMAy-b-DEGMAz, and b) Pluronic® F127 (storage modulus, G', in blue, and loss modulus, G", in grey), and ii) SANS data of c) the novel polymer and b) Pluronic® F127, at selected temperatures. The SANS data of PEGMAx-b-BuMAy-b-DEGMAz were fitted by using the SasView software and i) an Elliptical Cylinder model with a hard sphere

at 23°C and 37°C and ii) a Broad Peak model at 47°C. The SANS data for Pluronic® F127 were fitted by using the IGOR software. Note: Data are plotted in a log-log scale.

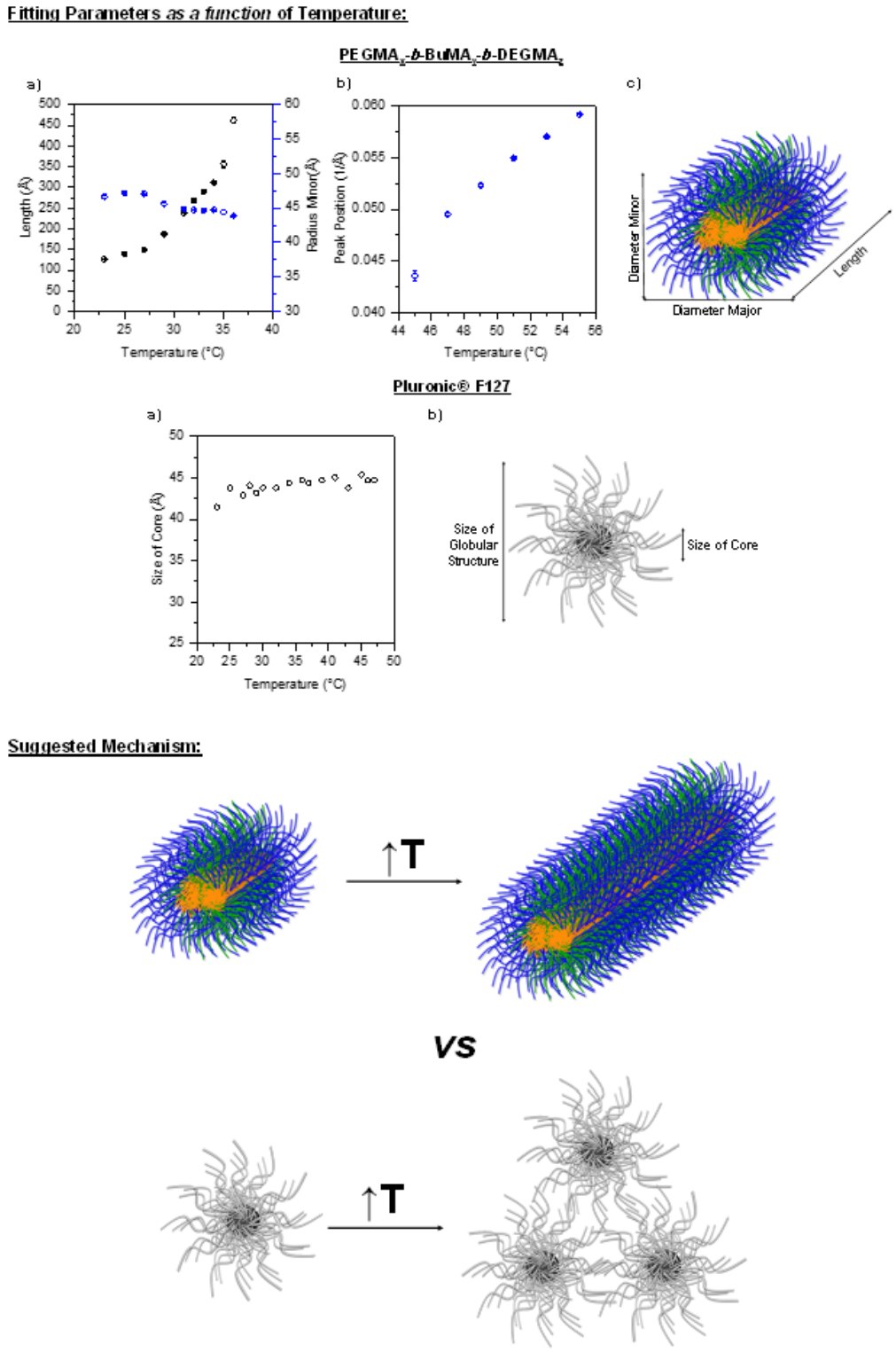

Figure 4

The fitting parameters of the self-assembled structures as a function of temperature for: PEGMAx-b-BuMAy-b-DEGMAz (top panel) – a) length or radius minor vs temperature, b) peak position vs temperature, and iii) micelle structure adopted by PEGMAx-b-BuMAy-b-DEGMAz, in which blue, orange

and green represent the hydrophilic, hydrophobic and thermoresponsive blocks, respectively, Pluronic® F127 (middle panel) – a) size of core vs temperature and ii) globular structure adopted by Pluronic® F127, where grey and black correspond the hydrophilic and hydrophobic blocks, respectively. The proposed mechanisms of gelation are schematically illustrated (bottom panel).

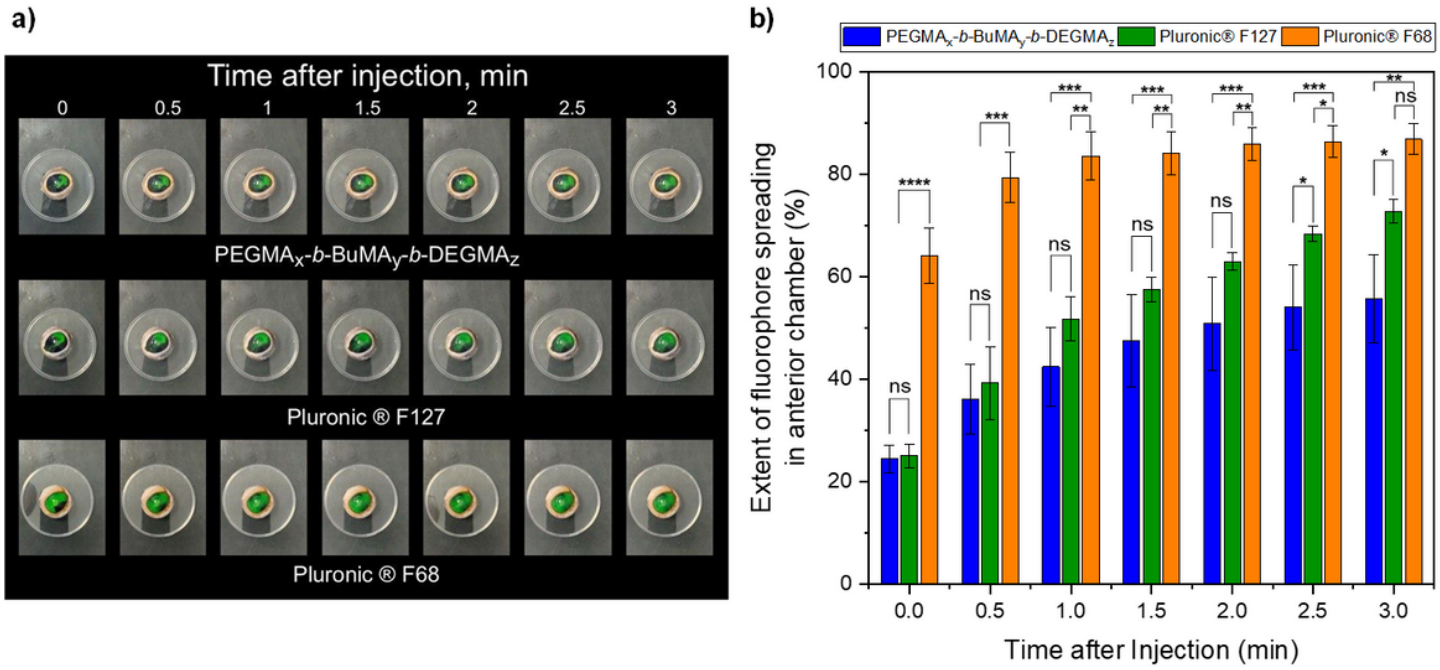

Figure 5

Ex vivo intracameral injections of 15 wt % PEGMAx-b-BuMAy-b-DEGMAz, Pluronic® F127 and Pluronic® F68 solutions, containing 1 mg/mL sodium fluorescein, into freshly excised bovine eyes: images taken at different time intervals following intracameral injection (a) and extent of fluorophore spreading in anterior chamber as a function of time (b). Data are expressed as mean ± standard deviation (n = 3).

Supplementary Files

This is a list of supplementary files associated with this preprint. Click to download.

- ConstantinouPBDtriblockvsF127SANSstudySupplementaryNov2020submitted.docx